ORIGINAL PAPER

CrossMark

Enhanced electroactive phase, toughness and dielectric properties of poly(vinylidene fluoride) with addition of MMA-BA-IL copolymer

Shixin Song[1] · Xiujie Bi[1] · Shangkun Jiang[1] · Xue Lv[1] · Shulin Sun[1] · Quanming Li[2]

Abstract

Methyl methacrylate (MMA), butyl acrylate (BA) and 1-butyl-3-vinylimdazolium tetrafluoroborate ([BVIM][BF$_4$]) copolymer (MMA-BA-IL) was prepared and used to enhance the electroactive phase content, toughness and dielectric properties of poly(vinylidene fluoride) (PVDF). Fourier transform infrared spectroscopy (FTIR), X-ray diffraction (XRD) and differential scanning calorimetry (DSC) tests indicated that crystal transformation of PVDF from α-phase to β/γ-phase occurred due to ion-dipole interaction between PVDF and [BVIM][BF$_4$]. Scanning electron microscope (SEM) results showed MMA-BA-IL copolymer dispersed in the PVDF uniformly and the partial replacement of MMA components by [BVIM][BF$_4$] decreased the miscibility between PVDF and MMA-BA copolymer. MMA-BA-IL copolymer improved the tensile ductility and impact toughness of PVDF. When the content of MMA-BA-IL was beyond 10 wt%, the elongation at break was higher than 400% and the impact strength was higher than 600 J/m. Deformation mechanism researches proved that shear yielding of the PVDF matrix and debonding/cavitation of the MMA-BA-IL copolymer particles were the major toughening mechanisms. The addition of MMA-BA-IL copolymer enhanced the dielectric properties of PVDF significantly. When the MMA-BA-IL content was 15 wt%, the dielectric constant of the PVDF/MMA-BA-IL blend increased to 54.3 at the 100 Hz frequency, which improved by 246% relative to that of the pure PVDF.

Keywords Poly(vinylidene fluoride) · Ionic liquid copolymer · Electroactive phase · Toughness · Dielectric properties

Introduction

Researches on dielectric polymer composites have attracted widely interest due to their potential applications in sensor, actuator and energy storage fields [1–3]. Poly(vinylidene fluoride) (PVDF) has usually been used as a precursor to prepare PVDF-based dielectric materials due to its high dielectric constant and favorable flexibility [4–8]. The dielectric constant of PVDF is about 10, which is quite higher than most of the pure polymers but is still lower than electroactive crystals and dielectric ceramics. In order to achieve the applications, the improvement in the dielectric constant is one of the important issues [9, 10].

Some methods have been adopted to enhance the dielectric constant of PVDF. In general, dielectric ceramics and conductive fillers are usually applied to blend with PVDF and composites with high permittivity can be achieved. The dielectric ceramics, such as BaTiO$_3$, Zeolite and ZnO have successfully raised the dielectric constant of PVDF in some literatures [11–15]. However, the shortcoming for this way lies in the high volume addition of the ceramic which decreases the flexibility of the polymers and leads to environmental harm. As conductive fillers, carbon nanotube, graphite nanoplates and metals were introduced into PVDF matrix to achieve higher dielectric properties [16–20]. Although many investigations have been performed to increase the compatibility between PVDF and the conductive fillers, the uniform dispersion of the fillers in PVDF matrix is still a significant challenge. Furthermore, the conductive fillers can lead to higher leakage current and result in higher dielectric loss.

✉ Shulin Sun
sunshulin1976@163.com

✉ Quanming Li
liquanmingjl@163.com

[1] Engineering Research Center of synthetic resin and special fiber, Ministry of Education, Changchun University of Technology, Changchun 130012, China

[2] Key Laboratory of Automobile Materials, College of Materials Science & Engineering, Jilin University, Changchun 130025, China

Table 1 Composition of the PVDF/MMA-BA blends

Designation used here	PVDF/IL0–1	PVDF/IL0–3	PVDF/IL0–5	PVDF/IL0–7	PVDF/IL0–10	PVDF/IL0–15
PVDF content (wt%)	99	97	95	93	90	85
MMA-BA content (wt%)	1	3	5	7	10	15

Recently, the blends of PVDF and ionic liquids (ILs) attracted the interest of some researchers [21–28]. ILs show many excellent properties such as high ionic conductivity, high thermal and chemical stabilities, strong polarity, low toxicity and a broad electrochemical potential window. The investigations about PVDF and ILs blends were focused on the crystalline structure, miscibility, transparency, physical properties and electrical conductivity. Due to the high ionic conductivity, ILs should be used as conductive fillers to improve the dielectric properties of PVDF. S. Lanceros-Mendez's group prepared PVDF/IL composites by solvent casting and melting method [21–23]. They pointed out that the charge structure of ionic liquid reduced the crystallinity and resulted in the complete piezoelectric β phase crystallization of PVDF. The PVDF/IL composites displayed lower elastic modulus due to the plastification effect of ILs and showed excellent displacement and bending under applied voltage, which was beneficial to be used as electromechanical actuators. Li's group prepared PVDF/IL composites by melt mixing and electron beam irradiation method [24–28]. They found that ILs showed excellent miscibility with PVDF and the composites displayed outstanding ductility, antielectrostatic and optical properties [24]. On the other hand, electron beam irradiation caused the grafting of unsaturated ILs onto the PVDF chains which improved the dielectric permittivity and decreased the dielectric loss of the composites [25, 26]. Furthermore, the PVDF/IL nanocomposites with conductive carbon black and multiwalled carbon nanotubes were also prepared to further improve the properties of the blends and these materials show promising for use in dielectric capacitor applications [27, 28]. In our group, 1-butyl-3-vinylimdazolium tetrafluoroborate ([BVIM][BF$_4$]) was used as ionic liquid to in-situ copolymerized with methyl methacrylate (MMA) in poly(vinylidene fluoride) (PVDF) solution by the free radical polymerization method. The introduction of [BVIM][BF$_4$] into the in-situ PVDF/P(MMA-co-[BVIM][BF$_4$]) composites enhanced the electrical conductivity and dielectric constant of PVDF [29].

In the present paper, methyl methacrylate (MMA), butyl acrylate (BA) and 1-butyl-3-vinylimdazolium tetrafluoroborate ([BVIM][BF$_4$]) copolymer (MMA-BA-IL) were prepared by the emulsion polymerization method. PMMA has been proved to be completely miscible with PVDF. The use of MMA as comonomer is to improve the miscibility of the copolymer with PVDF. The BA section can improve the toughness of the blends. The IL component can enhance the dielectric properties of PVDF. Furthermore, polymerized MMA, BA and [BVIM][BF$_4$] integrate in the form of macromolecular structure, which improves the stability of [BVIM][BF$_4$] in the composite and decreases the dielectric loss of the PVDF/MMA-BA-IL blends. It was found that the addition of (MMA-BA-IL) promoted the improvement of electroactive phase content, toughness and dielectric properties of PVDF. The PVDF/MMA-BA-IL composites show potential applications in sensor, actuator and energy storage fields.

Materials and methods

Materials

PVDF (Solef 6010, made in France) was commercially purchased from Dongguan Wenjin New Materials Co. Ltd., China. MMA and BA were kindly provided by Jilin Chemistry Company, China. The ionic liquid (IL), 1-butyl-3-vinylimdazolium tetrafluoroborate [BVIM][BF$_4$], was obtained from Shanghai Cheng Jie Chemical Co. Ltd., China. Hexadecane (HD) was purchased from Acros. Tween 80 was supplied by Meryer (Shanghai) Chemical Technology Company and used as received. Tetrahydrofuran was purchased from Beijing Chemistry Reagents Company. 2, 2-azobisisobutyronitrile (AIBN) was supplied by Shanghai Chemistry Reagent Company, China. Deionized water was used in all experiment processes.

Table 2 Composition of the PVDF/MMA-BA-IL blends

Designation used here	PVDF/IL20–1	PVDF/IL20–3	PVDF/IL20–5	PVDF/IL20–7	PVDF/IL20–10	PVDF/IL20–15
PVDF content (wt%)	99	97	95	93	90	85
MMA-BA-IL content (wt%)	1	3	5	7	10	15

Fig. 1 The FTIR results of PVDF and its blends: **a** PVDF/MMA-BA, **b** PVDF/MMA-BA-IL
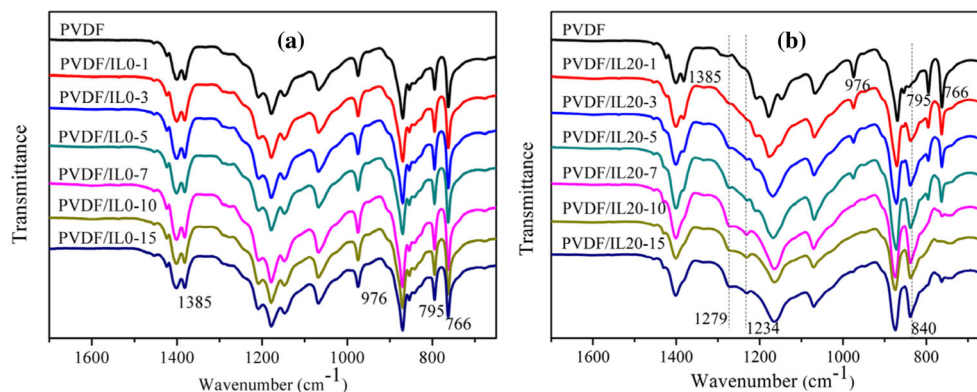
Preparation of MMA-BA-IL copolymer

The MMA-BA-IL copolymer was synthesized by emulsion polymerization method. The oil mixture including MMA, BA, IL, HD and AIBN were stirred 1 h under nitrogen. The water phase including water and Tw80 (emulsifier) also were stirred 1 h under nitrogen. After agitation, the oil and water phases were combined together and stirred 1 h for pre-emulsification and homogenized by ultrasonication for 10 min under cooling with an ice-water bath. The polymerization was carried out for 5 h at 70 °C in a 3-neck 500 ml round bottom glass reaction flask with a Teflon stirring paddle and a Friedrichs condenser under N_2 atmosphere. The copolymer was isolated from the emulsion by drying in a vacuum oven at 60 °C for 24 h before being used. The monomer composition for the preparation of MMA-BA-IL copolymer is 30:50:20. Furthermore, the copolymer of MMA-BA was also prepared for comparison with MMA-BA-IL copolymer. The monomer composition for the preparation of MMA-BA copolymer is 50:50.

Blending and molding procedures

The melt blending of the PVDF/MMA-BA and PVDF/MMA-BA-IL blends was performed on a Thermo Haake mixer (Thermo Scientific, Karlsruhe, Germany) at 55 rpm and 200 °C for 5 min. The compositions of the blends are listed in Tables 1 and 2. After blending, samples with different compositions were obtained by hot press molding for 5 min at 200 °C and cold press molding for 3 min at room temperature.

Characterizations

Crystal phase tests

Crystal phases were characterized by Fourier transform infrared spectroscopy (FTIR) and X-ray diffraction (XRD) tests. The thickness of the samples is around 1 mm. FTIR

measurement was recorded from 650 cm^{-1} to 4000 cm^{-1} with a resolution of 4 cm^{-1} and 32 cm^{-1} scans. The XRD was measured on a D/MAX 2000/PC from 5° to 60° at a scanning speed of 10°min^{-1}.

DSC test

The melting behavior of the samples was tested with a Perkin-Elmer DSC-7 (Perkin-Elmer, Waltham, MA, USA). The samples were heated from 30 to 220 °C at 10 °C/min under a nitrogen atmosphere to test the melting behavior and held for 3 min at 220 °C to remove the thermal history, then cooled at a rate of 10 °C/min to 30 °C.

Mechanical tests

The notched Izod impact strength was tested by an XJU-22 Izod impact tester (Chengde Tester Machinery Factory, Chengde, China) at 23 °C according to ASTM D256. The dimensions of each sample were 63.5mm×12.7mm×3.18 mm, with a notch depth of 2.54 mm. The tensile tests were performed with an Instron-3365 tensile tester (Instron, Boston, MA, USA) according to ASTM D638 at a crosshead speed of 50 mm/min at 23 °C.
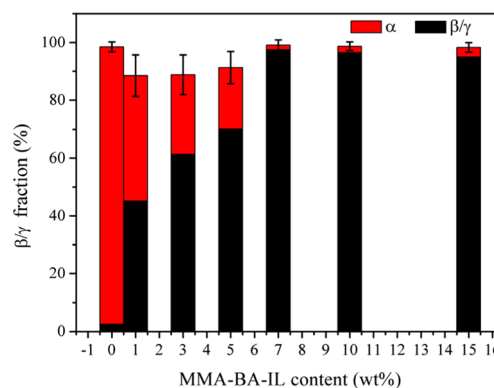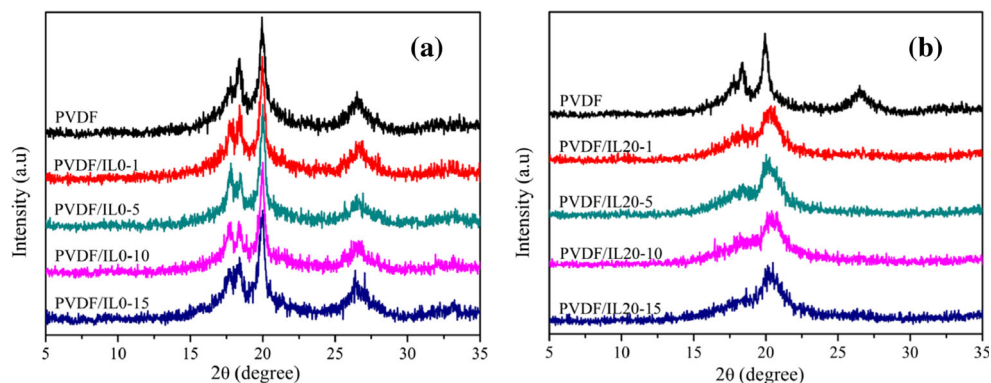

Fig. 2 The α-phase and β/γ-phase content calculated according to the FTIR results

Fig. 3 The XRD results of PVDF and its blends: **a** PVDF/MMA-BA, **b** PVDF/MMA-BA-IL

Morphology observation

Scanning Electron Microscopy (SEM) micrographs were characterized using a JSM6510 scanning electron microscope (JEOL, Tokyo, Japan). Before testing, all samples were coated with a gold layer for SEM observation with an operation voltage of 10 kV.

Dielectric properties

Dielectric measurements were performed on LCR Meter (E4980A, Keysight Technologies, USA) with the frequency ranging from 20 Hz to 2 MHz at room temperature. The samples were coated with silver paste before test. Thus the dielectric constant and dielectric loss were tested.

Results and discussion

Crystallization properties

PVDF shows several crystalline phases and at least five possible types of crystal phase, such as nonpolar α-phase, polar β-phase and γ, δ, and ε phases have been reported. FTIR and XRD measurements were usually used to determine the crystal forms of PVDF and its blends [30]. Figure 1a shows the

FTIR results of PVDF and PVDF/MMA-BA blends. According to the researches, the peaks at 766, 795, 976, 855 and 1385 cm^{-1} are the characteristic peaks of nonpolar α-phase. The ones at 840 and 1279 cm^{-1} are the polar β-phase, while the peaks at 840 and 1234 cm^{-1} belong to the polar γ-phase. From Fig. 1a, it can be found that PVDF displays the nonpolar α-phase and the addition of MMA-BA has no influence on the α-phase of PVDF. Figure 1b shows the FTIR results of PVDF and PVDF/MMA-BA-IL blends. Different with MMA-BA, MMA-BA-IL copolymer affects the crystal phase of PVDF obviously. With the increase of MMA-BA-IL content in the blends, the characteristic peaks intensity of α-phase decreases and the characteristic peak intensity of β/γ-phase (840, 1234 and 1279 cm^{-1}) increases significantly. From the structure of MMA-BA and MMA-BA-IL, we can conclude that the transition from α to β/γ-phase is induced by IL composite.

The β/γ-phase content of the PVDF/MMA-BA-IL blends can be quantified from the FTIR spectra by the following equation [30, 31]:

$$F(\beta/\gamma) = \frac{A_P}{1.26A_{NP} + A_P}$$

A$_P$ and A$_{NP}$ correspond to the absorbance at 840 cm^{-1} (polar β/γ phase) and 766 cm^{-1} (non-polar α-phase), respectively. The relative β/γ-phase content is showed in Fig. 2. It

Fig. 4 Melting behaviors of PVDF and its blends: **a** PVDF/MMA-BA, **b** PVDF/MMA-BA-IL
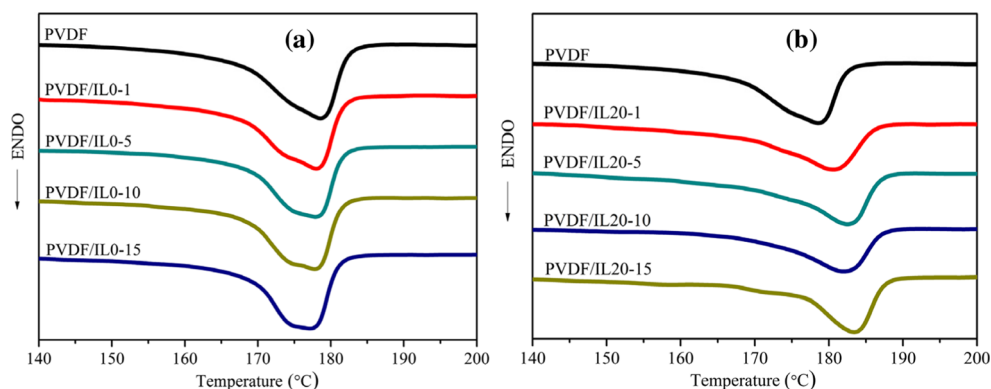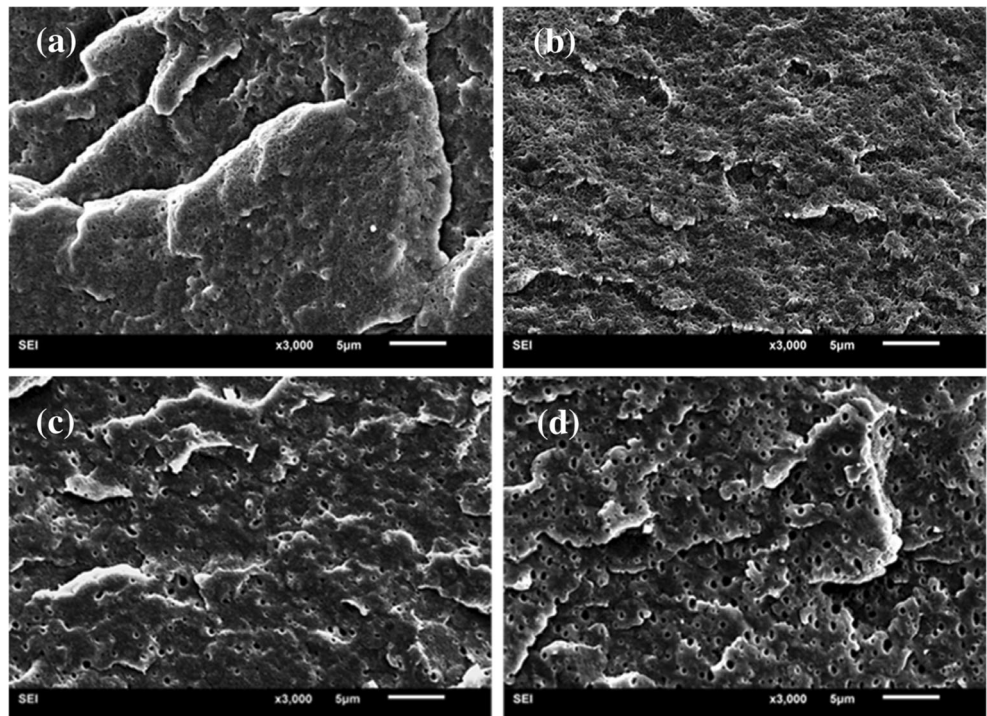
Fig. 5 The SEM results of PVDF/
MMA-BA (**a**: 5 wt% MMA-BA
copolymer, **b**: 10 wt% MMA-BA
copolymer) and PVDF/MMA-
BA-IL (**c**: 5 wt% MMA-BA-IL
copolymer, **d**: 10 wt%
MMA-BA-IL copolymer) blends after
etched

can be found that, when the content of MMA-BA-IL is more than 7 wt%, more than 95% α-phase transfers to β/γ-phase.

The crystal transformation can be further confirmed by the XRD result. Figure 3 showed the XRD curves of the pure PVDF and its blends. Pure PVDF exhibits characteristic diffraction peaks around 17.66, 18.30, 19.90 and 26.56°, which are ascribed to the (100), (020), (110) and (021) reflections of α-phase. As for the PVDF/MMA-BA blends, no crystal transition for PVDF can be found (Fig. 3 a). However, when IL is introduced into MMA-BA, the intensity of α characteristic diffraction peaks for PVDF decreases or disappears, furthermore, the emergence of the peak at 20.26° (β-phase) and 20.04°(γ-phase) replaces the peak at 19.90° (α-phase), which is attributed to the crystal transformation from α-phase to β/γ-phase of PVDF (Fig. 3 b). From the results of FTIR and XRD, it can be concluded that the incorporation of IL copolymer induces the crystal transformation of PVDF from α-phase to β/γ-phase. Some studies reported that the addition of surface charged fillers in PVDF matrix could work as crystallization directors to induce the crystallization transformation of PVDF from α-phase to β/γ-phase [21, 22, 32–34]. P. Martins investigated the influence of $NiFe_2O_4$ and $CoFe_2O_4$ ferrite nanoparticles on the electroactive phase of PVDF [32, 33]. The results indicated that strong static electro interactions between the magnetic particles with a negative charge on the surface and PVDF chains with the positive CH_2 induced the polymer chains to align on the surface of the nanoparticle in the extended conformation and therefore resulting in the formation of β/γ phase. Furthermore, they reported the effects of anionic, nonanionic and cationic surfactants coated $CoFe_2O_4$ on the phase crystallization of PVDF [34]. The results showed that the nuclear effect of negative charged $CoFe_2O_4$-SDS was

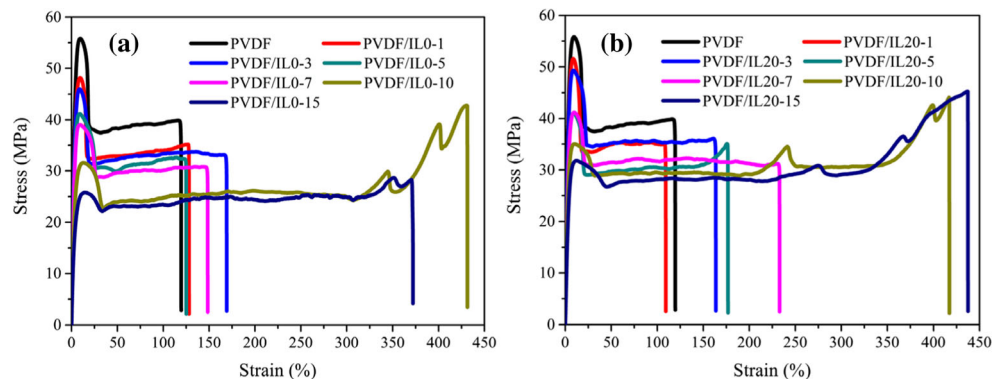**Fig. 6** The strain-stress curves of
PVDF and its blends: **a** PVDF/
MMA-BA, **b** PVDF/MMA-BA-
IL

Table 3   Mechanical properties of the PVDF/MMA-BA blends

Designation used here	PVDF	PVDF/IL0–1	PVDF/IL0–3	PVDF/IL0–5	PVDF/IL0–7	PVDF/IL0–10	PVDF/IL0–15
Impact strength (J/m)	165±11	195±8	209±13	309±12	649±9	660±9	824±25
Yield strength (MPa)	55.4±0.8	47.9±1.4	45.9±1.7	41.1±2.3	39.1±1.1	31.7±1.0	25.9±0.9
Break strength (MPa)	39.8±0.4	34.9±0.7	33.1±1.2	32.1±1.9	30.7±1.5	42.5±1.1	28.2±1.4
Elongation at break (%)	118±7	128±15	168±21	125±13	148±19	431±41	370±35

higher than that of zero surface charge $CoFe_2O_4$-Triton and positive charge $CoFe_2O_4$-CTAB. In addition, the effect of different ionic liquid anion and cation on the electroactive phase of PVDF was also investigated [22]. The results showed the incorporation of ILs into PVDF matrix promoted the increase of β/γ phase content due to the strong electrostatic interactions between the dipolar moments of PVDF and the ILs. Therefore, these works indicate that the phase crystallization of PVDF can be changed with the addition of negative charged fillers. As for the PVDF/MMA-BA-IL blends, the crystal transformation of PVDF from α-phase to β/γ-phase is mainly due to the existence of large number of negative ions in the copolymer. The strong electrostatic interactions between the positive CH_2 bonds of PVDF and the negative charges in ILs anion lead to preferential orientation of the polymer chains conformation corresponding to the β/γ phase.

DSC was used to identify the melting behavior of PVDF and the blends. It has been reported that the melting temperature of the α-phase is lower than that of the polar β and γ phases for PVDF [28, 35]. Figure 4 illustrates the DSC heating curves of pure PVDF and its blends. In Fig. 4 a, the pure PVDF exhibits a melting temperature at about 178.6 with a shoulder at lower temperature region. As for the PVDF/ MMA-BA blends (Fig. 4 a), the PVDF in the blends shows the similar melting temperature with the pure PVDF. On the other hand, the PVDF in the PVDF/MMA-BA-IL blends displays much higher melting temperature than the pure PVDF. The melting properties further prove the transition of α-phase to β/γ-phase of the PVDF in the PVDF/MMA-BA-IL blends due to the interaction between PVDF and IL.

Morphology properties

The phase morphology of polymer blends is very important for the property improvement and which is related with the miscibility between the different components. The miscibility between PVDF and PMMA has been investigated in detail [36]. The results showed that PVDF and PMMA were miscible and no phase separation occurred for PVDF/PMMA blends. Figure 5 a and b show the etched PVDF blends with 5 and 10 wt% MMA-BA copolymer. The MMA-BA components have been etched by tetrahydrofuran. It can be found that phase separation takes place for the PVDF/MMA-BA blends. On the other hand, the phase domain size is small and the particle size is similar between PVDF/PIL0–5 and PVDF/PIL0–10 blends. So PVDF shows good miscibility with MMA-BA copolymer due to the existence of MMA components. As for the PVDF/MMA-BA-IL blends, phase separation still can be found form the pictures of Fig. 5 c and d. Furthermore, compared with PVDF/MMA-BA blends, the PVDF/MMA-BA-IL blends display much larger phase domain size at the same copolymers content. So the partial replacement of MMA components by IL decreases the miscibility between PVDF and MMA-BA.

Mechanical properties

Figure 6 shows the typical strain-stress curves of the pure PVDF and its blends. The pure PVDF is rigid and displays higher yield stress and lower elongation at break than the blends. With the addition of MMA-BA or MMA-BA-IL copolymer, the yield strength of the blends decreases while the elongation at break increases obviously. When the content of MMA-BA or MMA-BA-IL copolymer is more than 10 wt%, the elongation at break is higher than 400% which is more than 3 times that of the pure PVDF. So the introduction of copolymers improves the ductility of PVDF. On the other hand, compared with PVDF/MMA-BA blends, the PVDF/ MMA-BA-IL blends show much higher yield strength and break strength when the copolymer content is the same, while

Table 4   Mechanical properties of the PVDF/MMA-BA-IL blends

Designation used here	PVDF	PVDF/IL20–1	PVDF/IL20–3	PVDF/IL20–5	PVDF/IL20–7	PVDF/IL20–10	PVDF/IL20–15
Impact strength (J/m)	165±11	194±13	202±15	288±21	625±10	652±9	807±31
Yield strength (MPa)	55.4±0.8	51.5±1.7	49.3±2.3	42.2±2.1	41.4±1.7	35.1±1.3	32.1±0.8
Break strength (MPa)	39.8±0.4	34.9±1.0	35.8±1.5	34.7±1.7	31.2±1.4	43.9±1.3	45.0±1.3
Elongation at break (%)	118±7	108±8	161±17	176±18	232±24	417±37	437±40

Fig. 7 Impact strength of PVDF and its blends: **a** PVDF/MMA-BA, **b** PVDF/MMA-BA-IL
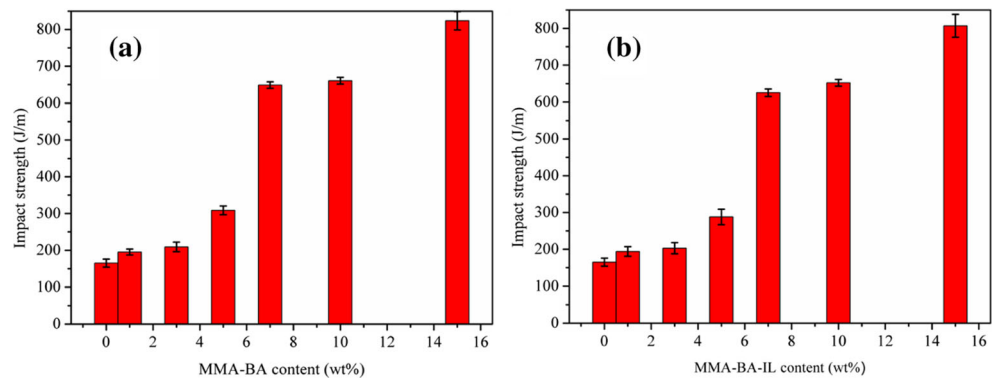
the elongation at break is similar. So PVDF/MMA-BA-IL blends maintain higher stiffness than PVDF/MMA-BA blends (see Tables 3 and 4).

Figure 7 shows the influence of MMA-BA or MMA-BA-IL copolymer content on the notched Izod impact strength of PVDF blends. The impact strength of PVDF is about 165 J/m. The impact strength of PVDF increases greatly with the addition of MMA-BA or MMA-BA-IL copolymer. Both MMA-BA and MMA-BA-IL perform good toughening ability for PVDF. The brittle-ductile takes place between 5 and 7 wt% copolymers content. On the other hand, no obvious difference exists between the toughening effect between MMA-BA and MMA-BA-IL. When the content of copolymers is higher than 7 wt%, the impact strength of the blends is higher than 600 J/m. So the blends show excellent impact toughness.

Figure 8 shows the deformation morphology of the impact fracture surface (a, b) and the deformation form under the impact fracture surface (c, d) for the PVDF blends. The pictures of the fracture surface (Fig. 8 a, b) show that obvious shear yielding occurs for the PVDF blends. At the same time, many cavities and copolymer particles can be found from the surface and some copolymer particles exist in the cavities. The morphology indicates that debonding between the PVDF matrix and copolymer particles has taken place and the much bigger cavities maybe formed by the agglomeration of some smaller cavities. Figure 8 c and d show the morphology under the fracture surface. The extensive shear yielding and cavities can also be found in the deformation zone. On the other hand, some small cavities also exist in the deformation zone which is due to the cavitation of the copolymer particles. So the shear yielding of the PVDF matrix and debonding/cavitation of the copolymer particles are the major energy absorption way, which promote the improvement of the toughness of PVDF blends.

Fig. 8 Fracture surface morphology of PVDF/MMA-BA-IL blends: **a** PVDF/IL20–5 and (**b**) PVDF/IL20–10; Morphology under the fracture surface of PVDF/MMA-BA-IL blends: **c** PVDF/IL20–5 and (**d**) PVDF/IL20–10
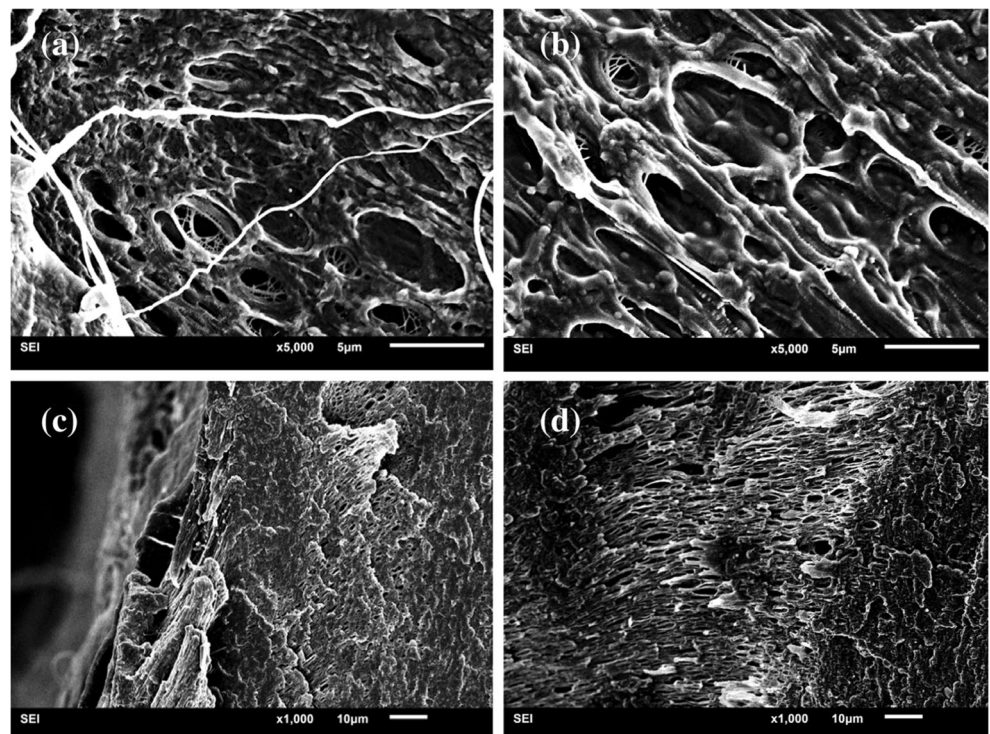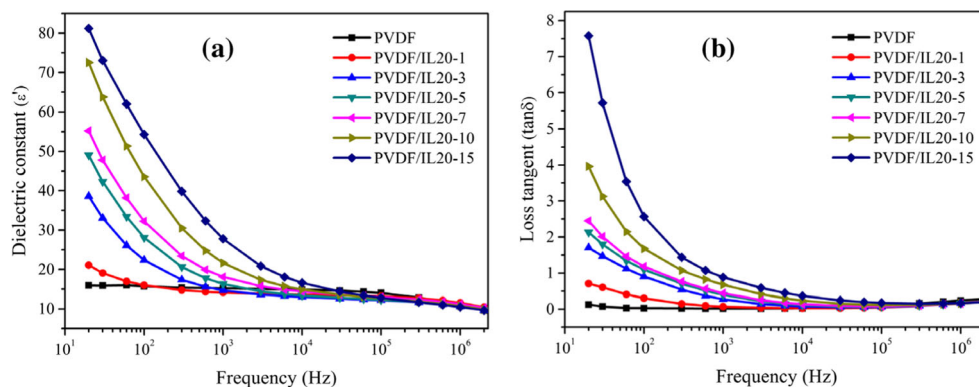
Fig. 9 The dielectric properties of PVDF and its blends: **a** dielectric constant, **b** loss tangent

Dielectric properties

Figure 9 shows the frequency dependence of dielectric properties of the pure PVDF and the PVDF/MMA-BA-IL blends at room temperature. It can be found that the dielectric properties of PVDF show weak dependence on frequency. With the addition of MMA-BA-IL copolymer, the dielectric constant and loss tangent of PVDF/MMA-BA-IL blends exhibit strong frequency dependence than that of PVDF. At low frequency, a similar feature of PVDF/MMA-BA-IL blends is that both dielectric constant and loss tangent increase along with the increase of MMA-BA-IL contents. The dielectric constant and loss tangent of PVDF/PIL20–15 blend are about 54.3 and 2.56 at the frequency of 100 Hz, which are much higher than pure PVDF. Similar phenomenon has been observed in ILs filled PVDF blends. The dielectric property and ionic conductivity are determined by the number and mobility of ions [21, 23, 37, 38]. For PVDF/MMA-BA-IL blends with high filler contents, large number of ions exists in the blends and exhibits high ion migration at low frequency, which lead to an increase in dielectric constant and loss tangent. However, with the further increase of frequency, a typical dielectric relaxation behavior occurs. In this situation, the speed of ions movement is lower than the electric field frequency switch and leads to low ion mobility in the blends. Therefore, the dielectric constant and loss tangent of PVDF/MMA-BA-IL blends decrease obviously at high frequency.

Conclusions

In the present research, emulsion polymerization was used to prepare methyl methacrylate (MMA), butyl acrylate (BA) and 1-butyl-3-vinylimdazolium tetrafluoroborate ([BVIM][BF$_4$]) copolymer (MMA-BA-IL). Due to the ion-dipole interaction between PVDF and IL ([BVIM][BF4]), the crystal of PVDF transformed from nonpolar α-phase to electroactive β/γ-phase and when the content of MMA-BA-IL is more than 7 wt%, more than 95% α-phase transfers to β/γ-phase.

SEM results indicated that BA-MMA and BA-MMA-IL showed good miscibility with PVDF and the copolymers distributed in the PVDF matrix uniformly. On the other hand, PVDF/MMA-BA-IL blends displayed much larger phase domain size than the PVDF/MMA-BA blends at the same copolymers content. So the partial replacement of MMA components by IL decreased the miscibility between PVDF and MMA-BA. The tensile ductility and impact toughness of PVDF were improved by MMA-BA-IL copolymer obviously. Shear yielding of the PVDF matrix and debonding/cavitation of the copolymer particles are the major energy absorption way, which promote the improvement of the toughness of PVDF blends. The dielectric properties of PVDF/MMA-BA-IL showed the frequency dependence. The dielectric constant of pure PVDF was 15.7 at 100 Hz frequency, while the dielectric constant of the PVDF/MMA-BA-IL blend increased to 54.3 at the same frequency, which increased by 246% relative to that of the pure PVDF. So in the present research, the electroactive β/γ-phase, ductility and dielectric properties of PVDF was improved significantly by the addition of MMA-BA-IL copolymer.

References

1. Zhang X, Shen Y, Xu B, Zhang Q, Gu L, Jiang J, Ma J, Lin Y, Nan CW (2016) Giant energy density and improved discharge efficiency of solution-processed polymer nanocomposites for dielectric energy storage. Adv Mater 28:2055–2061

2. Huang XY, Jiang PK (2015) Core-Shell structured high-k polymer nanocomposites for energy storage and dielectric applications. Adv Mater 27:546–554

3. Lin HJ, Li L, Ren J, Cai ZB, Qiu L, Yang Z, Peng HS (2013) Conducting polymer composite film incorporated with aligned carbon nanotubes for transparent, flexible and efficient supercapacitor. Sci Rep 3:1353

4. Roy S, Thakur P, Hoque NA, Bagchi B, Sepay N, Khatun F, Kool A, Das S (2017) Electroactive and high dielectric folic acid/PVDF

composite film rooted simplistic organic photovoltaic self-charging energy storage cell with superior energy density and storage capability. ACS Appl Mater Interfaces 19:24198–24209

5. Xia XD, Wang Y, Zhong Z, Weng GJ (2017) A frequency-dependent theory of electrical conductivity and dielectric permittivity for graphene-polymer nanocomposites. Carbon 111:221–230

6. Yang MH, Zhao H, He DL, Hu CH, Chen HW, Bai JB (2017) Carbon coated boron nitride Nanosheets for polymer nanocomposites with enhanced dielectric performance. Materials 10:741

7. Li R, Zhou J, Liu HJ, Pei JZ (2017) Effect of polymer matrix on the structure and electric properties of piezoelectric lead Zirconatetitanate/polymer composites. Materials 10:945

8. Su R, Lu ZD, Zhang DW, Liu Y, Wang ZP, Li JN, Bian JH, Li YX, Hu XH, Gao JH, Yang YD (2016) High energy density performance of polymer nanocomposites induced by designed formation of $BaTiO_3$@sheet-likeTiO$_2$ hybrid Nanofillers. J Phys Chem C 120:11769

9. Karan SK, Das AK, Bera R, Paria SA, Maitra N, Shrivastava K, Khatua BB (2016) Effect of γ-PVDF on enhanced thermal conductivity and dielectric property of Fe-rGO incorporated PVDF based flexible nanocomposite film for efficient thermal management and energy storage applications. RSC Adv 6:37773–37783

10. Thaku VK, Tan EJ, Lin MF, Lee PS (2011) Poly(vinylidene fluoride)-graft-poly(2-hydroxyethyl methacrylate): a novel material for high energy density capacitors. J Mater Chem 21:3751–3759

11. Xie LY, Huang X, Yang K, Li ST, Jiang PK (2014) "grafting to" route to PVDF-HFP-GMA/BaTiO$_3$ nanocomposites with high dielectric constant and high thermal conductivity for energy storage and thermal management applications. J Mater Chem A 2:5244–5251

12. Kim P, Jones SC, Hotchkiss PJ, Haddock JN, Kippelen B, Marder S, Perry JW (2007) Phosphonic acid-modified barium Titanate polymer nanocomposites with high permittivity and dielectric strength. Adv Mater 19:1001–1005

13. Kim P, Doss NM, Tillotson JP, Hotchkiss PJ, Pan MJ, Marder SR, Li JY, Calame JP, Perry JW (2009) High energy density nanocomposites based on surface-modified BaTiO$_3$ and a ferroelectric polymer. ACS Nano 3:2581–2592

14. Wang GS, Wu YY, Zhang XJ, Li Y, Guo L, Cao MS (2014) Controllable synthesis of uniform ZnO nanorods and their enhanced dielectric and absorption properties. J Mater Chem A 2:8644–8651

15. Li ZT, Zhang X, Li GH (2014) In situ ZnO nanowire growth to promote the PVDF piezo phase and the ZnO-PVDF hybrid self-rectified nanogenerator as a touch sensor. Phys Chem Chem Phys 16:5475–5479

16. Mohamadi S, Sharifi-Sanjani N, Foyouhi A (2013) Evaluation of graphene nanosheets influence on the physical properties of PVDF/PMMA blend. J Polym Res 20:1

17. Wang L, Dang ZM (2005) Arbon nanotube composites with high dielectric constant at low percolation threshold. Appl Phys Lett 87:284–291

18. Dang ZM, Wang L, Yin Y, Zhang Q, Lei QQ (2007) Giant dielectric Permittivities in functionalized carbon-nanotube/electroactive-polymer nanocomposites. Adv Mater 19:852–857

19. He F, Lau S, Chan HL, Fan JT (2010) High dielectric permittivity and low percolation threshold in nanocomposites based on poly(vinylidene fluoride) and exfoliated graphite Nanoplates. Adv Mater 21:710–715

20. Dang ZM, Lin YH, Nan CW (2003) Novel ferroelectric polymer composites with high dielectric constants. Adv Mater 15:1625–1629

21. Dias JC, Lopes AC, Magalhaes B, Botelho G, Silva MM, Esperanca JMSS, Lanceros-Mendez S (2015) High performance electromechanical actuators based on ionic liquid/poly(vinylidene fluoride). Polym Test 48:199–205

22. Mejri R, Dias JC, Lopes AC, Hentat SB, Silva MM, Botelho G, Ferro M, Esperanca JMSS, Maceiras A, Laza JM, Vilas JL, Leon LM, Lanceros-Mendez S (2015) Effect of ionic liquid anion and cation on the physico-chemical properties of poly(vinylidene fluoride)/ionic liquid blends. Eur Polym J 71:304–313

23. Mejri R, Dias JC, Lopes AC, Hentati SB, Marins MS, Costa CM, Lanceros-Mendez S (2016) Effect of anion type in the performance of ionic liquid/poly(vinylidene fluoride) electromechanical actuators. J Non-Cryst Solids 453:8–15

24. Xing CY, Zhao MM, Zhao LP, You JC, Cao XJ, Li YJ (2013) Ionic liquid modified poly(vinylidene fluoride): crystalline structures, miscibility, and physical properties. Polym Chem 24:5726–5734

25. Xing CY, Wang YY, Zhang C, Li LF, Li YJ, Li JY (2015) Immobilization of ionic liquids onto the poly(vinylidene fluoride) by Electron beam irradiation. Ind Eng Chem Res 38:9351–9359

26. Xing CY, You JC, Li YJ, Li JY (2015) Nanostructured poly(vinylidene fluoride)/ionic liquid composites: formation of organic conductive Nanodomains in polymer matrix. J Phys Chem C 36:21155–21164

27. Xing CY, Wang YY, Huang XY, Li YJ, Li JY (2016) Poly(vinylidene fluoride) nanocomposites with simultaneous organic Nanodomains and inorganic nanoparticles. Macromolecules 3:1026–1035

28. Xing CY, Zhao LP, You JC, Dong WY, Cao XJ, Li JY (2012) Impact of ionic liquid-modified multiwalled carbon nanotubes on the crystallization behavior of poly(vinylidene fluoride). J Phys Chem B 116:8312–8320

29. Bi XJ, Song SX, Sun SL (2017) Performance improvement of poly(vinylidene fluoride) by in situ copolymerization of methyl methacrylate and ionic liquid. Macromol Res 12:1–9

30. Martins P, Lopes AC, Lanceros-Mendez S (2014) Electroactive phases of poly(vinylidene fluoride): determination, processing and applications. Prog Polym Sci 4:683–706

31. Bahader A, Gui HG, Fang HG, Wang P, Wu SJ, Ding YS (2016) Preparation and characterization of poly(vinylidene fluoride) nanocomposites containing amphiphilic ionic liquid modified multiwalled carbon nanotubes. J Polym Res 6:184

32. Martins P, Costa CM, Lanceros-Mendez S (2011) Nucleation of electroactive β-phase poly(vinilidene fluoride) with $CoFe_2O_4$ and $NiFe_2O_4$ nanofillers: a new method for the preparation of multiferroic nanocomposites. Appl Phys A Mater Sci Process 1:233–237

33. Martin P, Costa CM, Benelmekki M, Botello G, Lanceros-Mendes S (2012) On the origin of the electroactive poly(vinylidene fluoride) β-phase nucleation by ferrite nanoparticles via surface electrostatic interactions. CrystEngComm 14: 2807–2811

34. Martins P, Caparros C, Gonçalves R, Martins PM, Benelmekki M, Botelho G, Lanceros-Mendes S (2012) Role of nanoparticle surface charge on the nucleation of the electroactive β-poly(vinylidene fluoride) nanocomposites for sensor and actuator applications. J Phys Chem C 116:15790–15794

35. Andrew JS, Clarke DR (2008) Enhanced ferroelectric phase content of polyvinylidene difluoride fibers with the addition of magnetic nanoparticles. Langmuir 16:8435–8438

36. Song HH, Yang SJ, Sun SL, Zhang HX (2013) Effect of miscibility and crystallization on the mechanical properties and transparency of PVDF/PMMA blends. Polym -Plast Technol Eng 52:221–227

37. Sencadas V, Lanceros-méndez S, Sabater iSR, Andrio BA, Gómez RJL (2012) Relaxation dynamics of poly(vinylidene fluoride) studied by dynamical mechanical measurements and dielectric spectroscopy. Eur Phys J E 35:41–52

38. Leones R, Costa CM, Machado AV, Esperança JMSS, Silva MM, Lanceros-Méndez S (2013) Development of solid polymer electrolytes based on poly(vinylidene fluoride-trifluoroethylene) and the [N$_{1 1 1 2(OH)}$][NTf$_2$] ionic liquid for energy storage applications. Solid State Ionics 253:143–150